

Article

Oilseed Rape Cultivars Show Diversity of Root Morphologies with the Potential for Better Capture of Nitrogen

László Kupcsik¹, Claudia Chiodi¹, Taraka Ramji Moturu¹, Hugues De Gernier^{1,†}, Loïc Haelterman¹, Julien Louvieaux^{1,2}, Pascal Tillard³, Craig J. Sturrock⁴, Malcolm Bennett⁴, Philippe Nacry³ and Christian Hermans^{1,*}

- ¹ Crop Production and Biostimulation Laboratory, Interfaculty School of Bioengineers, Université libre de Bruxelles, Campus Plaine CP 245, Bd du Triomphe, 1050 Brussels, Belgium; koopac@gmail.com (L.K.); claudia.chiodi@ulb.be (C.C.); taraka.ramji.moturu@ulb.be (T.R.M.); hugues.degernier@psb.vib-ugent.be (H.D.G.); loic.haelterman@ulb.be (L.H.); julien.louvieaux@ulb.be (J.L.)
- ² Laboratory of Applied Plant Ecophysiology, Haute Ecole Provinciale de Hainaut Condorcet, Centre pour l'Agronomie et l'Agro-industrie de la Province de Hainaut, 11 rue Paul Pastur, 7800 Ath, Belgium
- ³ Biochemistry and Plant Molecular Physiology, UMR 5004 CNRS/INRAE/SupAgro-M/UM2, Integrative Biology Institute for Plants, Place Viala, CEDEX 1, 34060 Montpellier, France; tillardp@orange.fr (P.T.); philippe.nacry@inrae.fr (P.N.)
- ⁴ Sutton Bonington Campus, School of Biosciences, University of Nottingham, Leicestershire LE12 5RD, UK; craig.sturrock@nottingham.ac.uk (C.J.S.); malcolm.bennett@nottingham.ac.uk (M.B.)
- * Correspondence: christian.hermans@ulb.be; Tel.: +32-2-650-5416
- † Present address: Department of Plant Biotechnology and Bioinformatics, Ghent University, 71 Technologiemark, 9052 Ghent, Belgium.



Citation: Kupcsik, L.; Chiodi, C.; Moturu, T.R.; De Gernier, H.; Haelterman, L.; Louvieaux, J.; Tillard, P.; Sturrock, C.J.; Bennett, M.; Nacry, P.; et al. Oilseed Rape Cultivars Show Diversity of Root Morphologies with the Potential for Better Capture of Nitrogen. *Nitrogen* **2021**, *2*, 491–505. <https://doi.org/10.3390/nitrogen2040033>

Academic Editors: Jacynthe Dessureault-Rompré and Marouane Baslam

Received: 1 October 2021
Accepted: 8 December 2021
Published: 14 December 2021

Publisher's Note: MDPI stays neutral with regard to jurisdictional claims in published maps and institutional affiliations.



Copyright: © 2021 by the authors. Licensee MDPI, Basel, Switzerland. This article is an open access article distributed under the terms and conditions of the Creative Commons Attribution (CC BY) license (<https://creativecommons.org/licenses/by/4.0/>).

Abstract: The worldwide demand for vegetable oils is rising. Oilseed rape (*Brassica napus*) diversifies cereal dominated crop rotations but requires important nitrogen input. Yet, the root organ is offering an untapped opportunity to improve the nitrogen capture in soil. This study evaluates three culture systems in controlled environment, to observe root morphology and to identify root attributes for superior biomass production and nitrogen use. The phenotypic diversity in a panel of 55 modern winter oilseed rape cultivars was screened in response to two divergent nitrate supplies. Upon in vitro and hydroponic cultures, a large variability for root morphologies was observed. Root biomass and morphological traits positively correlated with shoot biomass or leaf area. The activities of high-affinity nitrate transport systems correlated negatively with the leaf area, while the combined high- and low-affinity systems positively with the total root length. The X-ray computed tomography permitted to visualize the root system in pipes filled with soil. The in vitro root phenotype at germination stage was indicative of lateral root deployment in soil-grown plants. This study highlights great genetic potential in oilseed rape, which could be manipulated to optimize crop root characteristics and nitrogen capture with substantial implications for agricultural production.

Keywords: *Brassica napus*; natural variation; nitrogen nutrition; root system architecture

1. Introduction

Agriculture is facing the challenge of producing more food while reducing the negative environmental impact of nitrogen (N) fertilization. Synthetic N fertilizers come with elevated prices. Such costs are not only economical but also environmental, as fertilizers cause groundwater pollution by nitrate leaching [1,2] and air pollution by nitrous oxide emission [3,4]. Hence, there is a need to reduce the environmental footprint by lowering the fertilizer inputs. Breeding crops with greater Nitrogen Use Efficiency (NUE) is one solution to achieve that goal [5]. Agronomically, it is calculated as the ratio of crop yield to N units available. The NUE is a combination of the Nitrogen Uptake Efficiency (NUpE)—the ability of the crop to take up N from the soil and the Nitrogen Utilization Efficiency (NUtE)—the ability of the crop to utilize the absorbed N for producing yield [6,7]. The root system

architecture defines the spatial distribution of roots in the soil, which translates the ability of the plant to acquire soil resources [8]. At present, root-based approaches are being developed to improve NUE in various crops [9,10]. Still, methods for phenotyping crop root system architecture can be challenging.

Oilseed rape (*Brassica napus*) has poor NUE, with a low ratio of seeds produced per N unit applied [11]. Thus, improving NUE is essential to ensure the environmental and economic sustainability of that crop production [12,13]. Breeding programs are largely focusing on NUtE in above-ground organs [14–16] and research on soil and below-ground processes are limited [17]. Yet, the root organ holds potential for NUtE improvement [18,19]. Oilseed rape offers a large genetic diversity of root morphologies [20–23]. Nonetheless, literature on the influence of N nutrition on root growth and development in that crop is still scarce compared to parented *Arabidopsis thaliana*. In the model species, a dual effect of nitrate on lateral root development is described: (i) a systemic inhibition of uniformly elevated nitrate concentrations occurs on lateral root elongation at the post-emergence developmental stage and (ii) a localized stimulation of nitrate-rich patches triggers lateral root growth in a low N environment, known as the foraging capacity [24–27]. The exploitation of *Arabidopsis* has unveiled some molecular networks shaping root morphology in response to nutritional factors [28–32].

Several study cases showed that root morphology optimization results in greater plant productivity and increased nutrient stress tolerance [33,34]. A rapid root proliferation may be a determining factor for accessing N from deep layers of quickly leaching or drying soils [18]. The NUtE can be improved by redesigning a more branched root system that explores a larger soil volume to prevent N leaching [18,35]. There are indications that at low N supply, high-yielding oilseed rape cultivars are characterized by expansive root growth during the vegetative stage or after the flower stem extension [36,37] and by great N uptake [38]. These observations support the hypothesis that large root phenotypes may enhance N acquisition. Nevertheless, conflicting views may be expressed regarding a possible trade-off between profuse root system, contributing to the capacity of N uptake, and metabolic costs associated with the growth and maintenance of the root organ [39].

This study explores the natural variation of root morphology in response to the nitrate supply among a diversity panel of 55 modern winter oilseed rape cultivars. The technical objective was to set up and assess the relevance of three culture systems to observe root morphology at different growth stages. Eventually, we sought to strengthen the premise that (i) root biomass production and morphological traits could be positive indicators of above-ground biomass production and (ii) larger root system size would confer greater N uptake.

2. Materials and Methods

2.1. Plant Material

Seeds of 55 winter oilseed rape cultivars were obtained from the Walloon Agricultural Research Centre (CRA-W), Gembloux, Belgium. The description of these lines is given in Table S1.

2.2. In Vitro Culture and 2D Root Morphology Analysis

The in vitro culture was conducted in a growth chamber at a constant temperature of 21 °C and a photoperiod of 16 h light (40 $\mu\text{mol photons m}^{-2} \text{s}^{-1}$)/8 h darkness. Seeds of 55 cultivars were sterilized in 2 mL microtubes after sequentially adding 70% (*v:v*) ethanol for 10 min, 20% (*v:v*) hypochlorite solution for 5 min and rinsing twice with sterile water. Then, seeds were plated on square (12 cm \times 12 cm) dishes filled with a modified Murashige-Skoog (MS) medium containing 0.010 mM KNO_3 + 9.090 mM KCl (hereby referred as low nitrate treatment, N⁻) or 10 mM KNO_3 (high nitrate, N⁺) and 2% (*w:v*) plant agar (Duschefa, Haarlem, the Netherlands) [40,41]. Seeds were stratified during two days at 4 °C. After three days, seedlings were transferred to a fresh growth medium of identical composition. The top portion (~3 cm) of the agar medium was cut and four

seedlings were inserted between the gel matrix and the bottom of the plate (Figure 1a). Three plates containing four seedlings per cultivar and per N condition were prepared. Seedlings grew during four days prior to harvest, corresponding to seven days after germination. Root and shoot organs were separated and dried at 60 °C. The pooled dry weights of four organs from one plate were measured. For root morphology observation, the dishes were scanned at a resolution of 400 dpi. The scans were annotated using the RootNav image analysis software [42].

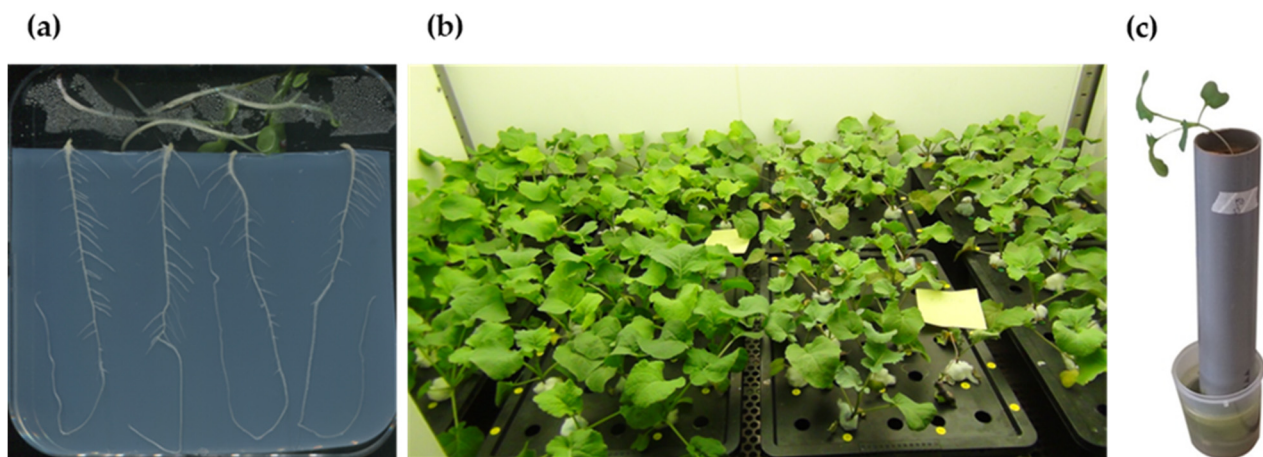


Figure 1. Culture systems used to grow oilseed rape cultivars. (a) Vertically placed agar plates (size: 12 cm × 12 cm); (b) Hydroponic containers (capacity: 8 L); (c) Column filled with soil (d: 5 cm, h: 30 cm).

2.3. Hydroponic Culture, Physiological Characterization, and Nitrate Uptake Assays

The hydroponic culture was performed in a growth chamber at a constant temperature of 20 °C, a photoperiod of 8 h light ($150 \mu\text{mol photons m}^{-2} \text{s}^{-1}$)/16 h darkness and a relative humidity of 60%. First, seeds of 12 selected cultivars were sown in peat-based soil (DCM Maison et Jardin, EAN:5413448070033) and stratified during two days at 4 °C. After five days, the roots were carefully rinsed with water and seedlings transferred for seven days into hydroponic containers, with dimensions 35 cm × 25 cm × 13.5 cm and filled with 8 L of nutrient solution (Figure 1b). Plants were first fed during nine days with a nutrient solution containing 1 mM $\text{Ca}(\text{NO}_3)_2$ [43,44], then during seven days with solutions containing 0.1 mM $\text{Ca}(\text{NO}_3)_2$ + 1.9 mM CaCl_2 (N−) or 1 mM $\text{Ca}(\text{NO}_3)_2$ (N+). Five plants per cultivar and per N condition were cultivated. Plants were harvested after nine days of treatment, corresponding to 21 days after germination. Roots and leaves were separated and scanned at a resolution of 400 dpi. Total root lengths were measured with the image analysis software Optimas 6.0 (Meyer Instruments, Inc., Houston, TX, USA). Organs were dried at 60 °C and dry weight was measured. Between 10 and 50 mg of crushed organ samples were analyzed with a Vario MAX Cube (Elementar, Langenselbold, Germany) for simultaneous carbon and nitrogen determination at the Centre pour l’Agronomie et l’Agro-Industrie de la province de Hainaut (CARAH), 11 rue Paul Pastur, 7800 Ath, Belgium.

The ^{15}N labelling procedure for the nitrate uptake assay was conducted as described in [45]. Plants were fed during 21 days with a nutrient solution containing 1 mM $\text{Ca}(\text{NO}_3)_2$ [43,44]. Then, they were incubated for 90 min in a solution containing 0.1 mM or 5 mM KNO_3 . Roots were sequentially bathing for 1 min in 10 mL of CaSO_4 solution (0.1 mM), for 5 min in 10 mL of a solution containing 0.1 mM or 5 mM K^{15}NO_3 (Sigma-Aldrich, Saint-Quentin-Fallavier, France) and for 1 min in 10 mL CaSO_4 solution (0.1 mM). Root and shoot organs were immediately separated and dried at 60 °C, prior to dry weight measurement. Samples were analyzed with an integrated system for continuous flow isotope ratio mass spectrometry (Euro-EA elemental Analyzer, EuroVector IRMS Isoprime Elementar) at the

Stable Isotope Analytical platform of the Biochemistry and Plant Molecular Physiology, INRAE Montpellier, Place Viala, CEDEX 1, 34060 Montpellier, France.

2.4. Soil Culture and Micro-Scale Computed Tomography Imaging

The soil culture was conducted between 20 April and 18 May 2015, in a greenhouse located on the Sutton Bonington campus, Nottingham University (UK), with the control on light and temperature levels. Seeds of four selected cultivars were germinated in soil-filled pipes (d = 5 cm, h = 30 cm) for the purpose of X-ray computed tomography (Figure 1c). The soil was collected on a site (50°36'47'' N, 3°46'12'' E) without recorded agricultural activity during the last decades. The loamy soil characteristics were total C = 1.05%, organic N = 1.13‰, N-NH₄⁺ = 0.73 mg kg⁻¹, N-NO₃⁻ = 10.48 mg kg⁻¹, Ca = 224 mg 100 g⁻¹, K = 31.76 mg 100 g⁻¹, Mg = 10.89 mg 100 g⁻¹ and p = 16.08 mg 100 g⁻¹. The columns were watered from the top with 500 mL of a nutrient solution without nitrate (N-) or with 50 mM KNO₃ (N+) [43,44]. Watering was stopped two days prior to scanning. All images were acquired using a Phoenix v|tome|x m scanner (GE Measurement and Control Solutions, Billerica, MA, USA). The accelerating voltage was 150 kV and the current 160 µA. The X-rays were filtered through a 0.1 mm copper plate. For each sample, there were 4 × 2160 projections taken with an exposure time of 200 ms, and signal averaging of two and one skip per projection. These were then assembled into a single 3D image with a 58 µm spatial resolution. The root images were segmented and measured manually using VGStudio MAX.

2.5. Statistical Treatment

Analysis of variance for the in vitro and hydroponic culture dataset was performed using a linear model implemented with the lmer function in the {lme4} package in R statistical language. The model consisted of fixed effects for cultivar and nitrate treatment and their interactions. Pearson correlations were calculated for all combinations of phenotypic traits in every nitrate condition, using R and XLSTAT. The principal component analyses of the in vitro and hydroponic culture dataset were conducted with XLSTAT. The Tukey's Honesty Significant Difference (HSD) test for the nitrate uptake assay was performed using R.

3. Results

Biomass production and root morphology were examined in a set of 55 winter oilseed rape cultivars (Table S1). Three culture systems were employed to examine the root system in response to the nitrate supply. In a pilot screen, the full set grew in vitro (Figure 1a). Eventually, a dozen of cultivars with contrasting root morphologies were further characterized in hydroponics (Figure 1b), and four of them upon soil culture (Figure 1c).

3.1. Variation for Biomass Production and Root Morphologies in Seedlings Cultivated In Vitro

Seedlings grew on vertical dishes filled with agar medium, as illustrated in Figure 1a. The germination characteristics of seedlings grown with 0.01 mM (N-) or 10 mM (N+) nitrate are presented in Figure 2. In this case, 12 selected cultivars were ranked from the poorest to the greatest total root length at N-: Cardiff (CAR), SY Carlo (CLO), Exocet (EXO), NK Aviator (AVI), DK Exquisite (EXQ), Recordie (REC), Limone (LIM), SY Saveo (SAV), Hertz (HER), Troy (TRO), Battz (BAT) and ES Jason (JAS). On average for the diversity panel cultivated in vitro, the root biomass (R, +28%) and the root-to-shoot biomass ratio (R:S, +39%) were superior, while the shoot biomass (S, -18%) and the total biomass (R + S, -8%) were inferior at N- compared to N+. The length of primary root (L_{PR}, +18%), the lengths of primary root zone 2 and zone 4 (L_{Z2} and L_{Z4}, +24%), the number of lateral roots (N_{LR}, +38%), the sum of lateral root lengths (ΣL_{LR}, +63%), the total root length (TLR, +41%), the density of lateral roots in zone 1 (D_{LR-Z1}, +22%) and the specific root length (SRL, +15%) increased, while the length of primary root zone 3 (L_{Z3}, -351%) and the density of lateral

roots in zone 2 (D_{LR-Z2} , -8%) decreased at $N-$ compared to $N+$ treatment. The cultivars showed considerable variation for biomass production and root morphology in response to N supply (Figure 3a,b). Variations for N_{LR} and ΣL_{LR} were generally the largest ones, and they were amplified at $N+$ compared to $N-$. For instance, the percentage differences for ΣL_{LR} between extreme cultivars were more than ten-fold (CAR vs. JAS at $N-$ and CLO vs. LIM at $N+$). The responsiveness of one cultivar to N depletion (i.e., increase/decrease of one trait value in response to $N-$ compared to $N+$) was evaluated (Figure 3c). A large variation in lateral root phenotypic plasticity was observed, with cultivars being poorly (CAR showing ΣL_{LR} increase less than 10%) or greatly (BAT showing ΣL_{LR} increase more than 500%) responsive to $N-$. The genotype (cultivar) effect, the environment (N treatment) effect and the interaction (cultivar \times N) were significant ($p < 0.05$) for all traits, except the (cultivar \times N) for S biomass (ns) (Table S2). The in vitro observations highlight an important variability among cultivars in terms of root morphological traits, and this leaves space for genetic selection targets in breeding programs.

A principal component analysis was used to compress and classify the biomass and root morphology data (Figure 4a,b). The two first principal components (PCs) explained together 71% of the total phenotypic variation. The PC1 (53.1%) was influenced the most by root morphological traits, while PC2 (17.8%) by the shoot biomass production (Figure 4a). The distribution of the cultivars across PC1 and PC2 permitted to clearly distinguish between the two N treatments (Figure 4b). Cultivars with low PC1 scores exhibited long primary and lateral roots, while those with elevated PC2 scores produced important aerial biomass.

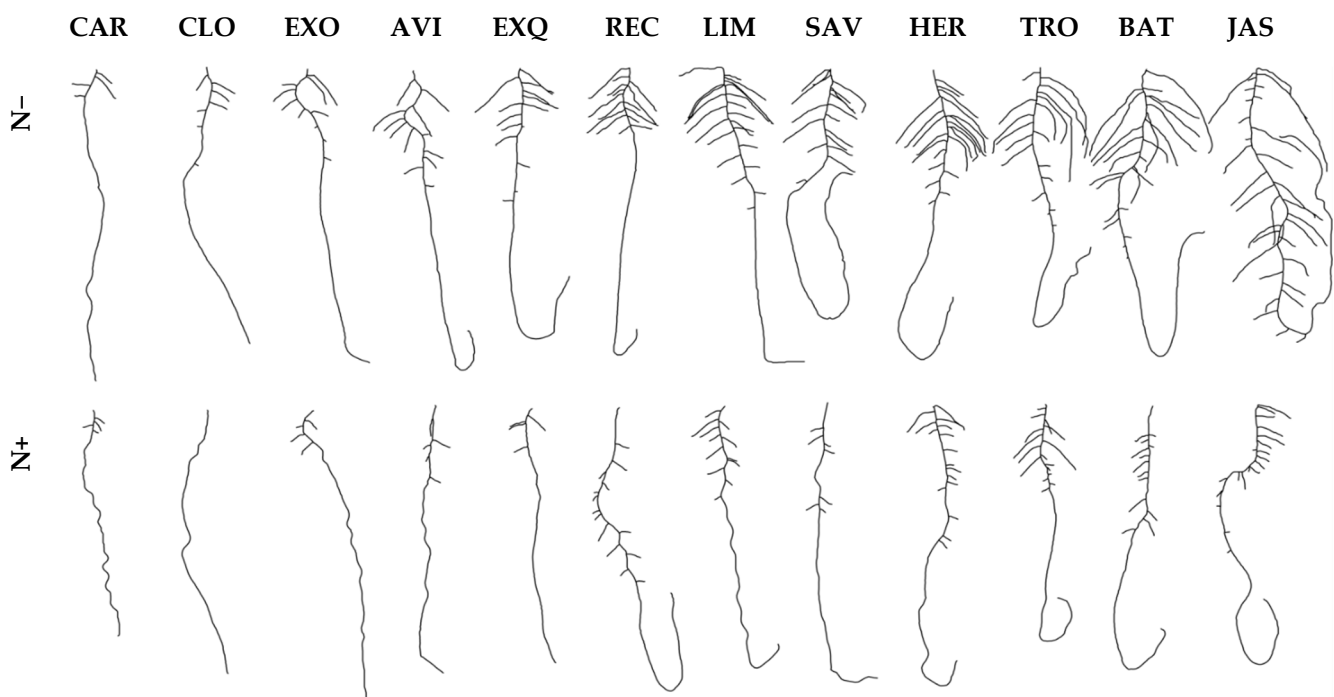


Figure 2. Root morphologies of oilseed rape cultivars grown in vitro with two divergent nitrate supplies. Pictures of representative root organs of 12 contrasting oilseed rape accessions grown with 0.01 mM (upper row, $N-$) or 10 mM (lower row, $N+$) nitrate supplies. Accessions are ranked from the left to the right by increasing total root length (TRL) measured at $N-$. The TRL values were ranging between 12.1 ± 0.9 cm (CAR) and 41.5 ± 2.9 cm (JAS). Cultivar full names are listed in Table S1. Scale bar: 2 cm.

Spearman correlation coefficients were calculated between the traits measured in vitro (Figure S1). Some correlations were found between derivative traits and their components (Table 1) but also between unrelated traits. The strongest and most significant correlation was found between L_{PR} and $\sum L_{LR}$ ($\rho^2 = 0.57$; $p < 0.001$) at N-. Furthermore, S biomass showed weak but significant positive correlations with N_{LR} and $\sum L_{LR}$ ($0.15 < \rho^2 < 0.26$, $p < 0.001$) during both N treatments.

Table 1. Abbreviations and definitions of the measured traits.

Biomass Production	
R	Root biomass
S	Shoot biomass
R + S	Total biomass
R:S	Root to shoot biomass ratio
Root Morphology	
L_{PR}	Length of primary root; $L_{PR} = L_{Z2} + L_{Z3} + L_{Z4}$
L_{Z2}	Length of primary root zone 2, between the first and last lateral roots; = 0 if $N_{LR} = 0$ or $N_{LR} = 1$
L_{Z3}	Length of primary root zone 3, between the hypocotyl junction and the first lateral root; = L_{PR} if $N_{LR} \leq 1$
L_{Z4}	Length of primary root zone 4, between the last lateral root and the primary root tip; = 0 if $N_{LR} \leq 1$
N_{LR}	Number of lateral roots > 1 mm
$\sum L_{LR}$	Sum of lateral root lengths
TRL	Total root length; = $L_{PR} + \sum L_{LR}$
D_{LR-Z1}	Density of lateral roots in zone 1; = N_{LR}/L_{PR}
D_{LR-Z2}	Density of lateral roots in zone 2; = $(N_{LR}-1)/L_{Z2}$, not defined if $N_{LR} \leq 1$
SRL	Specific root length; = $(L_{PR} + \sum L_{LR})/R$
Shoot Morphology	
LA	Leaf area
SLA	Specific leaf area; = LA/S
Carbon and Nitrogen Analyses	
C_R	Carbon concentration in root tissues
C_S	Carbon concentration in shoot tissues
N_R	Nitrogen concentration in root tissues
N_S	Nitrogen concentration in shoot tissues
NUI	Nitrogen utilization index; = $S/((S \times N_S) + (R \times N_R))$
Nitrate Uptake Assay	
$^{15}N_{QR}$	^{15}N amount in root tissues
$^{15}N_{QS}$	^{15}N amount in shoot tissues
$HATS/LATS \text{ plant}^{-1}$	HATS/LATS mediated ^{15}N influx rate per hour and per plant; = $(^{15}N_{QR} + ^{15}N_{QS})/5 \times 60$
$HATS/LATS \text{ root biomass}^{-1}$	HATS/LATS mediated ^{15}N influx rate per hour and per root biomass; = $(^{15}N_{QR} + ^{15}N_{QS})/5 \times 60 \times R$

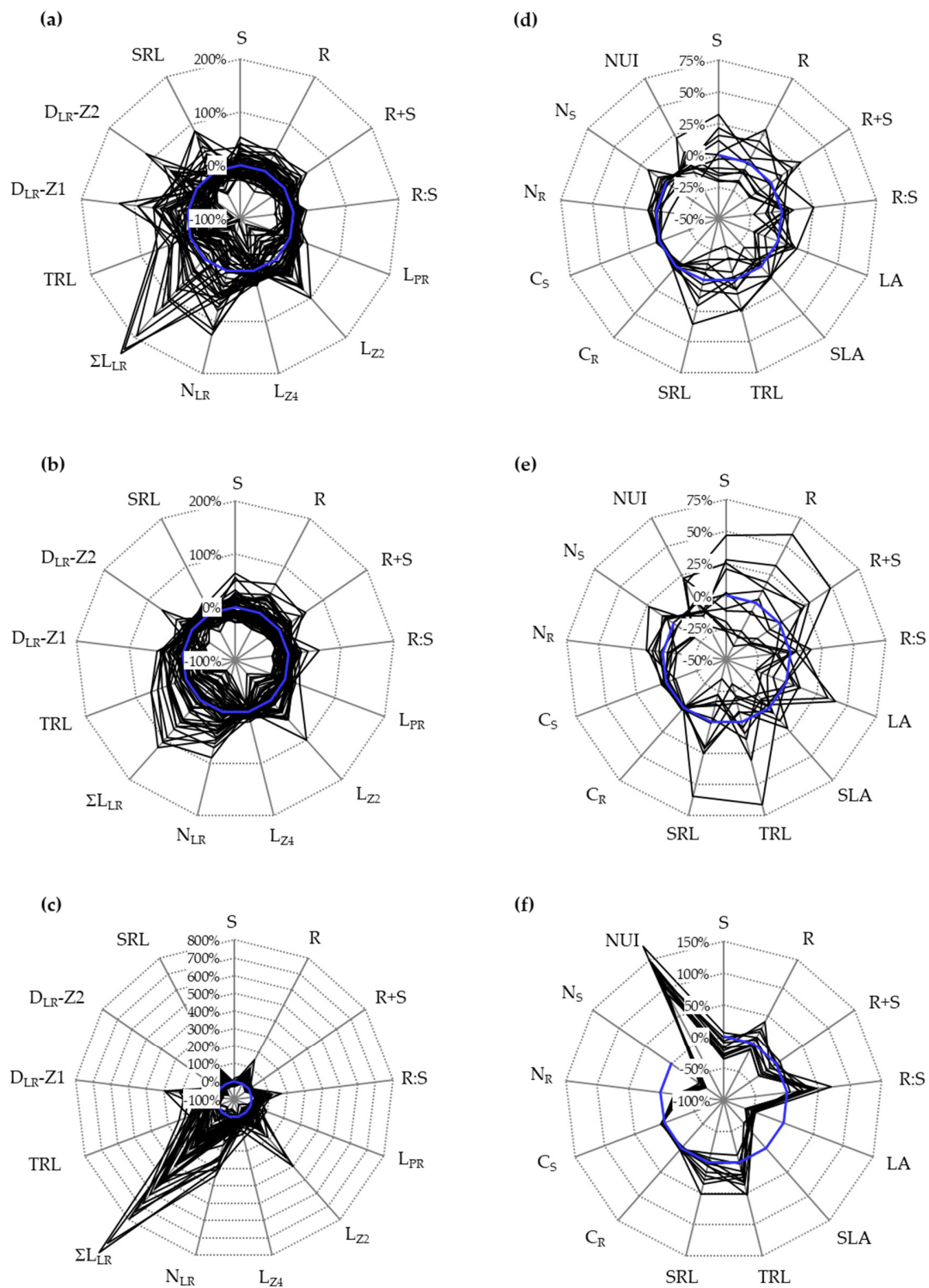


Figure 3. Relative variation of phenotypic traits measured in 55 oilseed rape cultivars cultivated in vitro (**a–c**) and in 12 cultivars in hydroponics (**d–e**). The spider plots (**a,b,d,e**) show the percentage variation of a given trait for every cultivar, normalized by the mean value of the panel, measured during N+ (**a,d**) or N– (**b,e**) conditions. Zero percent (blue circle) indicates no difference compared to the mean value of the panel in one condition. The spider plots (**c,f**) show the percentage variation of a given trait for every cultivar grown during N–, normalized by the value observed during N+ conditions. This defines the responsiveness of one trait to nitrate depletion. Zero percent (blue circle) indicates no difference compared to elevated nitrate conditions. $n = 15$ plants per genotype and per N condition cultivated in vitro, and 5 plants in hydroponics. Traits are defined in Table 1.

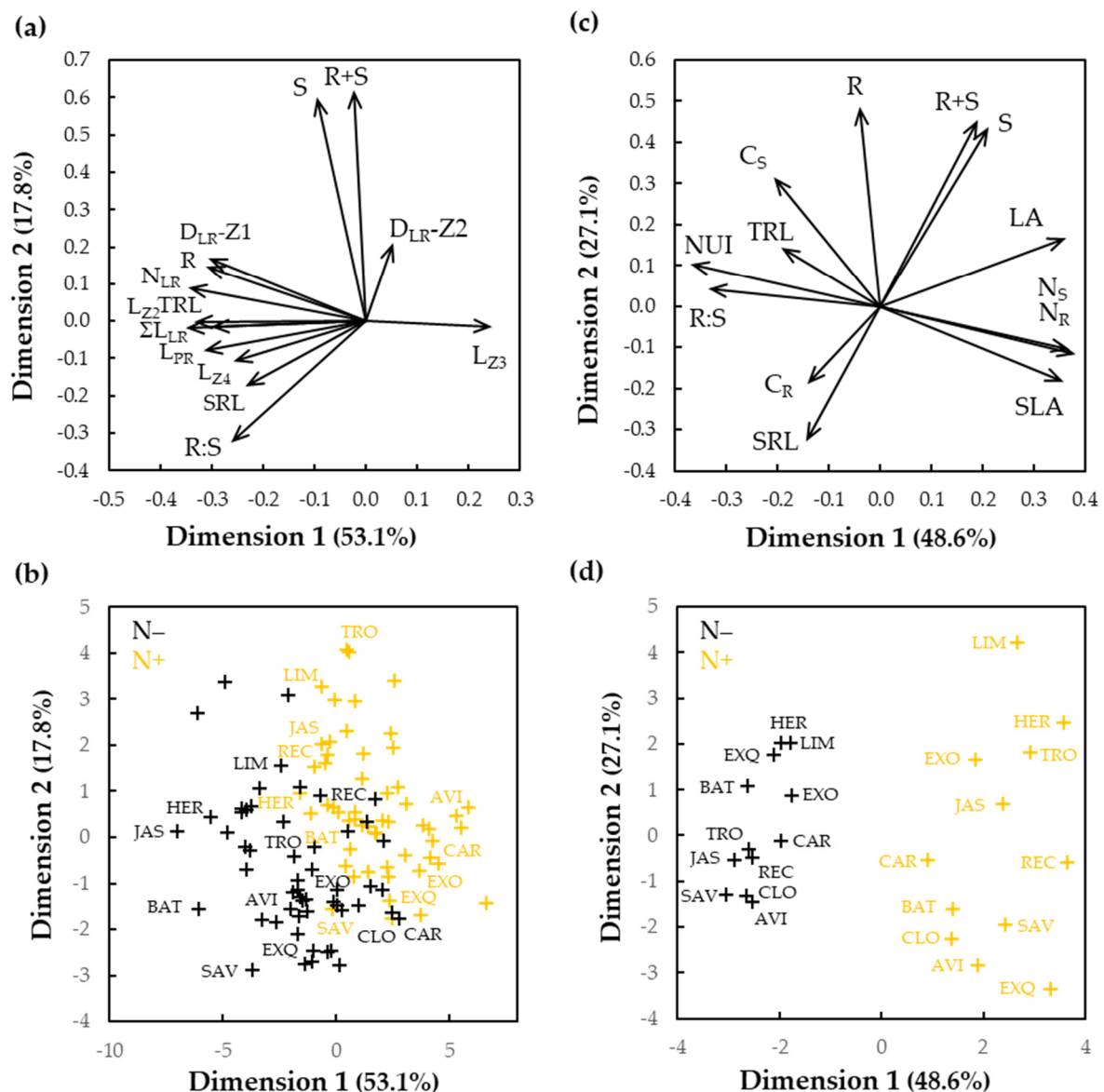


Figure 4. Principal component analysis of 14 phenotypic traits measured in 55 oilseed rape cultivars cultivated in vitro (a,b) and of 13 phenotypic traits in 12 cultivars in hydroponics (c,d). (a,c) Principal component (PC) biplot showing the compositions of the first two PCs, with cumulative variance; (b,d) Representation of the cultivars. Symbols indicate position of the cultivars as determined by their trait values in the two first PCs. Black symbols refer to low nitrate (N⁻) and yellow symbols to high nitrate (N⁺) conditions. Traits are defined in Table 1 and cultivars listed in Table S1.

3.2. Characterization of Selected Cultivars in Hydroponics

The vertical plate culture system delivered a rapid and extensive examination of 2D root morphology at seed germination. Next, we examined how these early observations were relating with later developmental stages. Based on the total lateral root length observed in vitro (see above), 12 contrasting cultivars were retained for further physiological analysis upon hydroponic culture (Figure 1b). Plants were fed with a nutrient solution containing 0.2 mM (N⁻) or 2 mM (N⁺) nitrate. On average for the core set cultivated in hydroponics, R (+7%) and R:S (+26%) were superior, whereas S (−24%) and R + S (−20%) were inferior at N⁻ compared to N⁺ (Table S3). The leaf area (LA) (−117%) and the specific leaf area (SLA) (−66%) decreased, while TRL (+18%) and SRL (+10%) increased in the same conditions. The nitrogen concentration in root tissues (N_R) (−36%) and in shoot tissues (N_S) (−154%) decreased, while the carbon concentration in root tissues (C_R) (+1%) and in shoot tissues (C_S) (+3%) increased. The nitrogen utilization index (NUI), used as a

surrogate for the nitrogen use efficiency at a vegetative stage, increased by 56%. They were large biometric variations between cultivars (Figure 3d,e). For instance, the percentage differences between the two most extreme cultivars were in the range of 34% (AVI and REC vs. LIM) and 65% (AVI vs. HER) for LA, and of 52% (CAR vs. BAT) and 82% (EXQ vs. BAT) for TRL, respectively, at N⁻ and N⁺. The responsiveness of cultivars to N depletion was also assessed (Figure 3f). A large variation in phenotypic plasticity was observed, with cultivars poorly or greatly responsive to N treatment for LA (e.g., SAV and TRO vs. RC) and TRL (e.g., CAR vs. BAT). The cultivar effect for all traits, the N treatment effect for all traits except R and NS, the interaction (cultivar × N) for all traits except R, S, SLA and TRL were significant ($p < 0.05$) (Table S3).

The two first PCs explained together three quarters of the total phenotypic variation. The PC1 (48.6%) was influenced the most by root morphological traits, while PC2 (27.1%) by the shoot biomass production (Figure 4c). The distribution of the cultivars across PC1 and PC2 permitted to clearly distinguish between the two N treatments (Figure 4d). Cultivars with low PC1 scores exhibited large leaves with elevated N concentration in tissues, while those with elevated PC2 scores produced important root biomass. We noted that the data collected from seedlings grown on vertical plates (Figure 4a,b) and those from plants grown in hydroponics (Figure 4c,d) showed the same pattern of response to the nitrate supply. The notable effect of N starvation was mainly reflected on R:S biomass ratio, TRL and SRL.

Spearman correlation coefficients were calculated between the traits measured in hydroponics (Figure S2). The strongest correlation was found between R and S biomasses ($\rho^2 = 0.63$ at N⁻, $\rho^2 = 0.95$ at N⁺). The SLA correlated negatively with C_S ($\rho^2 = -0.59$ at N⁻, $\rho^2 = -0.87$ at N⁺) and NUI ($\rho^2 = -0.79$ at N⁻, $\rho^2 = -0.76$ at N⁺), and positively with N_S ($\rho^2 = 0.72$ at N⁻, $\rho^2 = 0.77$ at N⁺). At N⁺, the LA correlated positively with R ($\rho^2 = 0.88$) and S ($\rho^2 = 0.77$). At N⁻, C_R correlated negatively with C_S ($\rho^2 = -0.66$), and SRL positively with N_R ($\rho^2 = 0.61$). All reported correlations are significant ($p < 0.001$).

A nitrate influx assay with ¹⁵N tracer was performed to assess the relationship between uptake capacity of roots and plant morphological traits. The activities of the nitrate High-(HATS) and Low-(LATS) Affinity Transport Systems were measured in 10 cultivars grown in hydroponics at N⁺ (Figure 5).

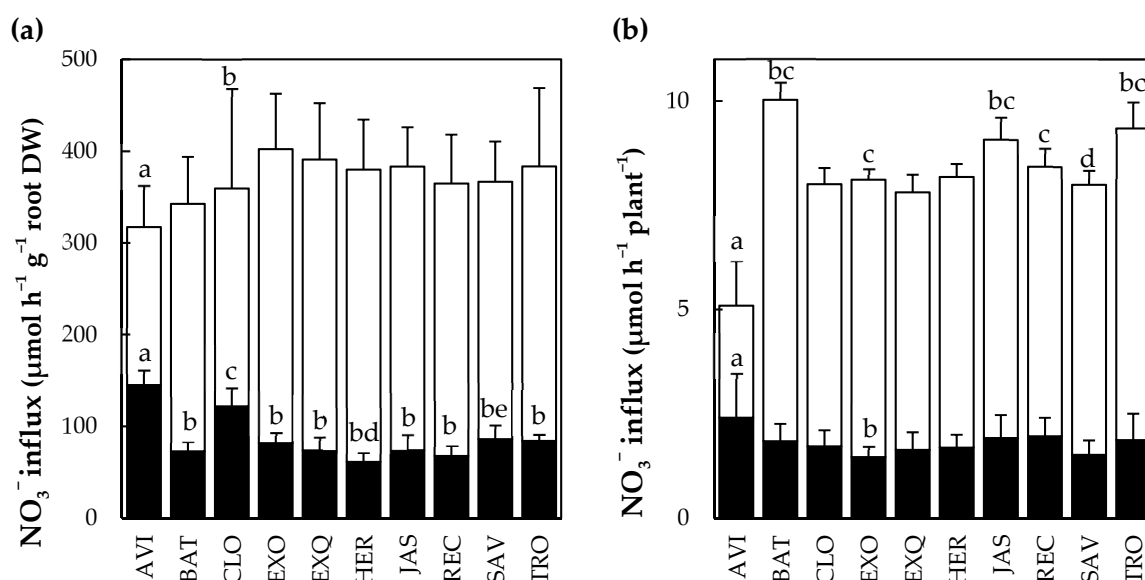


Figure 5. Variability of HATS and combined HATS and LATS activities between oilseed rape cultivars. (a) Nitrate influx expressed per hour and per root biomass. (b) Nitrate influx expressed per hour and per plant. Black bars: HATS activity, white bars: HATS + LATS activity. N = 6–12 plants ± std. Bars with different letters are significantly different ($p < 0.05$) according to Tukey's HSD test.

The HATS expressed per root biomass were four-fold less important than the HATS and LATS combined values. Variations between cultivars were in the range of 200% for HATS and 25% for HATS + LATS. The AVI and CLO cultivars had significant ($p < 0.05$) greater HATS values expressed per root biomass (Figure 5a). The AVI and BAT showed, respectively, the lowest and greatest HATS + LATS values expressed per plant (Figure 5b). The HATS expressed per root biomass was negatively correlated with LA ($\rho^2 = -0.74$; $p < 0.01$), while the HATS + LATS expressed per plant was positively correlated with TRL ($\rho^2 = 0.59$; $p < 0.05$) (Figure S3).

3.3. In-Soil Root Phenotyping

The X-ray computed tomography was used to examine the root system architecture of four cultivars (BAT, CLO, HER and SAV) in pipes filled with soil (Figure 1c). The profile of lateral roots along the taproot was assessed after watering with a solution without (N−) or with 50 mM KNO₃ (N+) (Figure 6). The CLO cultivar was showing poor soil exploration along with poor shoot development (data not shown), and it was weakly responsive to the N treatment. It may indicate that the culture conditions were particularly unfavorable for that cultivar. On the contrary, the lateral root deployment of BAT, HER and SAV was more profuse and concentrated close to the soil surface. The root system of the BAT cultivar was repressed in the upper soil portion, while the one of SAV was clearly stimulated by N− condition. The HER genotype showed subtle profile change in response to N treatment. There was no obvious difference close to the surface but less lateral root branching down to the pipe, during N− in that cultivar.

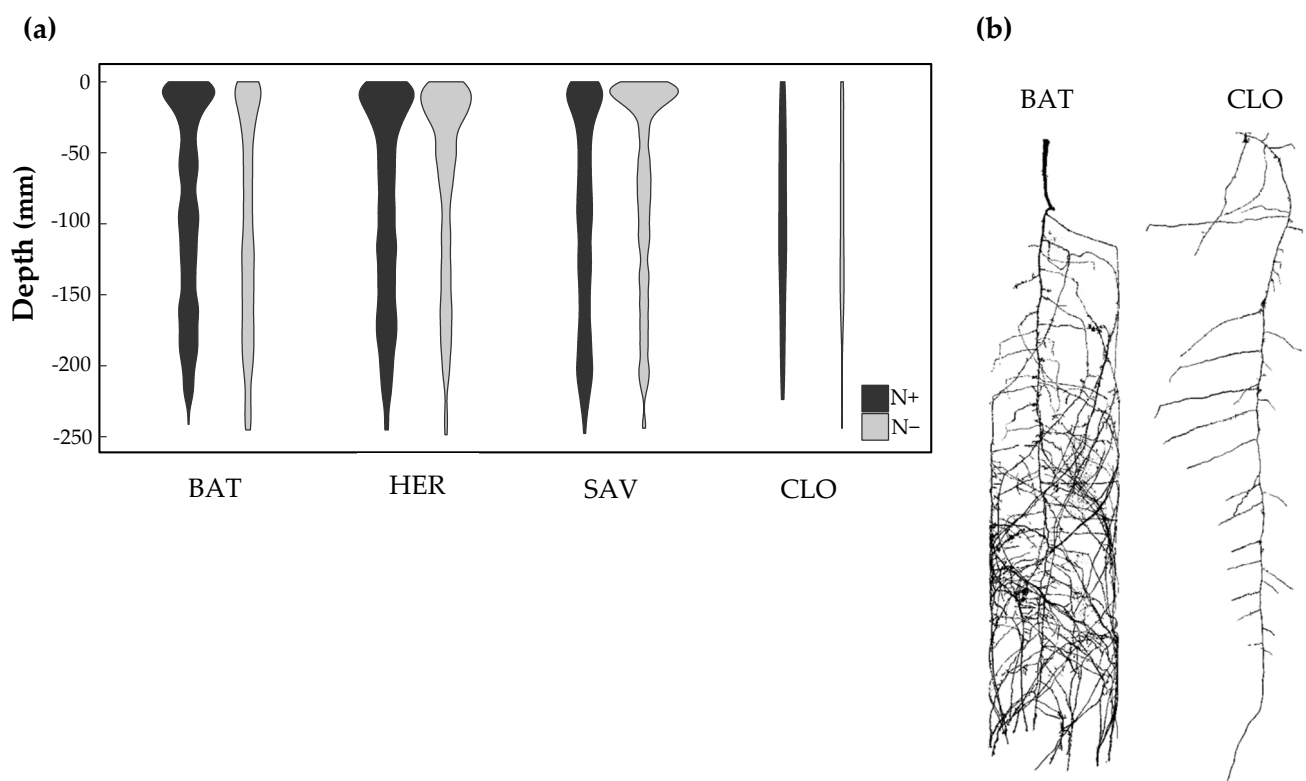


Figure 6. Characterization of the root system architecture in soil-filled column. (a) The violin plots show the distribution of lateral root density, as a function of the column depth. The estimates are based on five replicates of four oilseed rape cultivars cultivated with low (N−) or high (N+) nitrate conditions; (b) Reconstructed images of two contrasting cultivars at N−. Scale bar = 5 cm.

4. Discussion

Increasing NUE is essential to ensure the environmental and economic sustainability of oilseed rape production. Nonetheless, NUE is notoriously difficult to work with and

this is due to the many peripheral processes being involved. The root system is still considered as a 'black box' and very few studies have focused on oilseed rape root response to N supply. Indeed, the below-ground organ has been poorly considered in breeding programs. Today, it is recognized as a lever to improve soil resources uptake and to reduce the negative environmental impact of mineral fertilization [35,46–48]. A diversity panel of modern winter oilseed rape cultivars was challenged with divergent nitrate supplies to identify contrasting root morphologies. Such a screening strategy in laboratory conditions may speed up for breeders, the delivery of genotypes with desired root morphological features. However, given the complexity of the agricultural environment, these data obtained in laboratory conditions may not ultimately reflect the field situation [18].

In the quest for root phenotyping methods, we employed three different procedures in controlled environment and evaluated their practical values and limitations.

- (i) The *in vitro* culture system on vertical agar plate in sterile conditions, is a reliable approach for germinating seeds and observing two-dimensional root morphology. We have adapted the system, which is conveniently used for *Arabidopsis* model [41,49], to the more vigorous growth of oilseed rape (Figure 1a). That method is low cost but handling agar plates and analyzing scanned images are two laborious tasks. Despite, some algorithms could be used to speed up the extraction of root morphological traits from image data [50]. Finally, agar plate for culturing sprouts constitutes one first step towards further characterization of later developmental stages.
- (ii) The hydroponic culture in containers filled with nutrient solution (Figure 1b), is suitable for mineral nutrition studies. That culture system without substrate gives easy access to clean root organs, for physiological and molecular characterization data [51,52]. While plant biometrics (e.g., biomass and total root surface) can easily be monitored over time, no such detailed analysis of root morphological traits can be provided.
- (iii) The technique based on X-ray computed tomography allows to visualize the three-dimensional structure of the root system [48,53,54]. We recovered the segmentation of the main root and first-order lateral roots of four oilseed rape cultivars in a column filled with soil (Figure 1c). That experimental setting is low throughput, as image capture and analysis are time-consuming. The technique relies on discriminating differences in X-ray attenuation between roots and soil matrix. In this case, distinguishing between water-filled pore space and fine roots quickly became a challenge. Hence, the technique only provides a qualitative assessment of the root system in a small size pipe. Nonetheless, this may constitute a final laboratory phase prior to field phenomics [48]. For a small number of cultivars, the root phenotype at germination during *in vitro* culture (Figure 2) was indicative of the root system deployment in the soil (Figure 6). However, these observations should be treated with caution, as studies in other crops (e.g., wheat) are reporting a lack of correlation between the root systems at a young developmental stage in the laboratory environment and at a reproductive stage in the field [55].

Overall, the three complementary culture systems permitted to observe wide phenotypic variation among the diversity panel and to discriminate between cultivars with contrasting behaviors. For example, the cultivar CLO was poorly performing across all experimental settings and N conditions, contrary to HER consistently demonstrating superior characteristics (Figures 2, 4 and 6).

Arabidopsis is a prime model organism for studying root biology. Fundamental knowledge can be translated to *Brassica* crops, which are genetically related [56,57]. The model species may serve as a resource base for studying root morphogenesis in response to N availability and N acquisition. We observed some similar root morphological responses between the two species, despite different root growth rates. Nitrate depletion stimulated the lateral root outgrowth of *Arabidopsis* [41] and oilseed rape (Figures 2 and 3) seedlings during *in vitro* culture on agar plates. However, the number of lateral roots varied less but

the length of primary root (mainly L_{Z4}) was more influenced by nitrate depletion in crop compared to *Arabidopsis*.

Learning about mechanisms of lateral root growth stimulation or repression by nitrate availability will help drawing strategies to optimize root system architecture. We aimed at observing the elaboration of root traits in oilseed rape cultivars and how this relates to biomass production and N capture. A premise is that root biomass production and morphological traits could be positive indicators of above-ground biomass production (and presumably yield). A rationale shared by several authors is that a branched root system that explores an important soil volume would limit nitrate leaching [18,58–61]. This study shows no negative correlation between root biomass production or total root length and shoot biomass production during *in vitro* and hydroponic cultures (Figures S1 and S2). Large root system deployed by BAT, JA and TRO, can support great shoot biomass production. Hence, selection for root and shoot biomass production under laboratory settings may be equally effective for improving yield.

Identifying oilseed rape cultivars with greater N capture is a pressing issue for reducing N loss in soil. This study demonstrates some potential for increased sustainability of oilseed rape production by targeting traits related to N uptake. An important variability degree for the root system size (Figure 3) and the N uptake capacity (Figure 5) was uncovered. This likely reflects no direct selection for root traits in breeding history of oilseed rape. A positive relationship was found between the total root length and the nitrate influx of HATS + LATS expressed per plant (Figure S3). This indicates that the N uptake capacity was to some extent, root-morphology dependent. Interestingly, the HATS expressed per root biomass correlated negatively with the leaf area (Figure S3). It is known that plants are modulating root N acquisition in response to shoot N demand, through long-distance mobile proteins and peptides [62,63]. That negative correlation suggests a feedback regulation of N products from the shoot on the root N uptake.

5. Conclusions

We illustrated that gel and liquid cultures rapidly deliver quantitative plant biometrics, and tomography a more qualitative outcome. The study revealed a large diversity of root morphologies and variability of N uptake capacities. These traits can be introgressed into one performant NUpE genotype possessing large root surface (e.g., HER cultivar), great N uptake rate per root mass (e.g., AVI, CLO) and reducing the adverse impact of N products on root uptake.

Supplementary Materials: The following are available online at <https://www.mdpi.com/article/10.3390/nitrogen2040033/s1>, Figure S1: Inter-trait phenotypic correlations in 55 winter oilseed rape cultivars grown *in vitro*, Figure S2: Inter-trait phenotypic correlations in 12 winter oilseed rape cultivars grown in hydroponics, Figure S3: Correlation between nitrate influxes and leaf area and total root length in 10 oilseed rape cultivars grown in hydroponics, Table S1: List of oilseed rape cultivars used in the study, Table S2: Statistical treatment for the data set measured *in vitro*, Table S3: Statistical treatment for the data set measured in hydroponics.

Author Contributions: Conceptualization and original draft preparation: C.H., L.K.; Investigation, methodology: C.H., C.J.S., H.D.G., J.L., L.K., M.B., P.N., P.T., T.R.M.; editing, C.C., L.H. All authors have read and agreed to the published version of the manuscript.

Funding: This research was funded by Fonds de la Recherche Scientifique (F.R.S.-FNRS) (MIS and PDR T.0116.19), and by European Plant Phenotyping Network (EPPN) (Grant Agreement No. 284443).

Institutional Review Board Statement: Not applicable.

Informed Consent Statement: Not applicable.

Data Availability Statement: The data presented in this study are available on request from the corresponding author.

Acknowledgments: L.H. and C.H. are, respectively, PhD fellow and research associate from F.R.S.-FNRS.

Conflicts of Interest: The authors declare no conflict of interest.

References

- Huang, T.; Ju, X.; Yang, H. Nitrate leaching in a winter wheat-summer maize rotation on a calcareous soil as affected by nitrogen and straw management. *Sci. Rep.* **2017**, *8*, 42247. [[CrossRef](#)] [[PubMed](#)]
- Mateo-Marín, N.; Quilez, D.; Isla, R. Utility of stabilized nitrogen fertilizers to reduce nitrate leaching under optimal management practices. *J. Plant Nutr. Soil Sci.* **2020**, *183*, 567–578. [[CrossRef](#)]
- Velthof, G.L.; Lesschen, J.P.; Webb, J.; Pietrzak, S.; Miatkowski, Z.; Pinto, M.; Kros, J.; Oenema, O. The impact of the Nitrates Directive on nitrogen emissions from agriculture in the EU-27 during 2000–2008. *Sci. Total. Environ.* **2014**, *468–469*, 1225–1233. [[CrossRef](#)]
- He, T.; Yuan, J.; Luo, J.; Wang, W.; Fan, J.; Liu, D.; Ding, W. Organic fertilizers have divergent effects on soil N₂O emissions. *Biol. Fert. Soils* **2019**, *55*, 685–699. [[CrossRef](#)]
- Sharma, L.K.; Bali, S.K. A review of methods to improve nitrogen use efficiency in agriculture. *Sustainability* **2018**, *10*, 51. [[CrossRef](#)]
- Moll, R.H.; Kamprath, E.J.; Jackson, W.A. Analysis and interpretation of factors which contribute to efficiency to nitrogen utilization. *Agron. J.* **1982**, *74*, 562–564. [[CrossRef](#)]
- Bouchet, A.-S.; Laperche, A.; Bissuel-Belaygue, C.; Baron, C.; Morice, J.; Rousseau-Gueutin, M.; Dheu, J.-E.; George, P.; Pinochet, X.; Foubert, T.; et al. Genetic basis of nitrogen use efficiency and yield stability across environments in winter rapeseed. *BMC Genet.* **2016**, *17*, 131. [[CrossRef](#)]
- Smith, S.; De Smet, I. Root system architecture: Insights from Arabidopsis and cereal crops. *Phil. Trans. R. Soc. B* **2012**, *367*, 1441–1452. [[CrossRef](#)] [[PubMed](#)]
- Garnett, T.; Conn, V.; Kaiser, B.N. Root based approaches to improve nitrogen use efficiency in plants. *Plant Cell Environ.* **2009**, *32*, 1272–1283. [[CrossRef](#)]
- Rosolem, C.A.; Ritz, K.; Cantarella, H.; Galdos, M.V.; Hawkesford, M.J.; Whalley, W.R.; Mooney, S.J. Enhanced plant rooting and crop system management for improving N Use Efficiency. *Adv. Agron.* **2017**, *146*, 205–239.
- Sylvester-Bradley, R.; Kindred, D.R. Analysing nitrogen responses of cereals to prioritize routes to the improvement of nitrogen use efficiency. *J. Exp. Bot.* **2009**, *60*, 1939–1951. [[CrossRef](#)]
- Han, M.; Okamoto, M.; Beatty, P.H.; Rothstein, S.J.; Good, A.G. The genetics of nitrogen use efficiency in crop plants. *Annu. Rev. Genet.* **2015**, *49*, 269–289. [[CrossRef](#)] [[PubMed](#)]
- Wang, J.; Dun, X.; Shi, J.; Wang, X.; Liu, G.; Wang, H. Genetic dissection of root morphological traits related to nitrogen use efficiency in *Brassica napus* L. under two contrasting nitrogen conditions. *Front. Plant Sci.* **2017**, *8*, 1709. [[CrossRef](#)]
- Girondé, A.; Etienne, P.; Trouverie, J.; Bouchereau, A.; Le Cahérec, F.; Lepout, L.; Orsel, M.; Niogret, M.-F.; Nesi, N.; Carole, D.; et al. The contrasting N management of two oilseed rape genotypes reveals the mechanisms of proteolysis associated with leaf N remobilization and the respective contributions of leaves and stems to N storage and remobilization during seed filling. *BMC Plant Biol.* **2015**, *15*, 59. [[CrossRef](#)]
- Koelin-Findeklee, F.; Becker, M.A.; van der Graaff, E.; Roitsch, T.; Horst, W.J. Differences between winter oilseed rape (*Brassica napus* L.) cultivars in nitrogen starvation-induced leaf senescence are governed by leaf-inherent rather than root-derived signals. *J. Exp. Bot.* **2015**, *66*, 3669–3681. [[CrossRef](#)]
- Han, Y.; Liao, J.; Yu, Y.; Song, H.; Rong, N.; Guan, C.; Lepo, J.E.; Ismail, A.M.; Zhang, Z. Exogenous abscisic acid promotes the nitrogen use efficiency of *Brassica napus* by increasing nitrogen remobilization in the leaves. *J. Plant Nutr.* **2017**, *40*, 18. [[CrossRef](#)]
- Williams, S.T.; Vail, S.; Arcand, M.M. Nitrogen Use Efficiency in parent vs. hybrid canola under varying nitrogen availabilities. *Plants* **2021**, *10*, 2364. [[CrossRef](#)] [[PubMed](#)]
- Louvieaux, J.; Leclercq, A.; Haelterman, L.; Hermans, C. In-field observation of root growth and nitrogen uptake efficiency of winter oilseed rape. *Agronomy* **2020**, *10*, 105. [[CrossRef](#)]
- Vazquez-Carrasquer, V.; Laperche, A.; Bissuel-Bélaygue, C.; Chelle, M.; Richard-Molard, C. Nitrogen Uptake Efficiency mediated by fine root growth early determines temporal and genotypic variations in Nitrogen Use Efficiency of Winter Oilseed Rape. *Front. Plant Sci.* **2021**, *12*, 641459. [[CrossRef](#)] [[PubMed](#)]
- Fletcher, R.S.; Mullen, J.L.; Heiliger, A.; McKay, J.K. QTL analysis of root morphology, flowering time, and yield reveals trade-offs in response to drought in *Brassica napus*. *J. Exp. Bot.* **2015**, *66*, 245–256. [[CrossRef](#)] [[PubMed](#)]
- Thomas, C.L.; Alcock, T.D.; Graham, N.S.; Hayden, R.; Matterson, S.; Wilson, L.; Young, S.D.; Dupuy, L.X.; White, P.J.; Hammond, J.P.; et al. Root morphology and seed and leaf ionic traits in a *Brassica napus* L. diversity panel show wide phenotypic variation and are characteristic of crop habit. *BMC Plant Biol.* **2016**, *16*, 214. [[CrossRef](#)] [[PubMed](#)]
- Thomas, C.L.; Graham, N.S.; Hayden, R.; Meacham, M.C.; Neugebauer, K.; Nightingale, M.; Dupuy, L.X.; Hammond, J.P.; White, P.J.; Broadley, M.R. High-throughput phenotyping (HTP) identifies seedling root traits linked to variation in seed yield and nutrient capture in field-grown oilseed rape (*Brassica napus* L.). *Ann. Bot.* **2016**, *118*, 655–665. [[CrossRef](#)]
- Zhang, Y.; Thomas, C.L.; Xiang, J.; Long, Y.; Wang, X.; Zou, J.; Luo, Z.; Ding, G.; Cai, H.; Graham, N.S.; et al. QTL meta-analysis of root traits in *Brassica napus* under contrasting phosphorus supply in two growth systems. *Sci. Rep.* **2016**, *6*, 33113. [[CrossRef](#)] [[PubMed](#)]

24. Sun, C.; Yu, J.; Hu, D. Nitrate: A crucial signal during lateral roots development. *Front. Plant Sci.* **2017**, *8*, 485. [[CrossRef](#)] [[PubMed](#)]
25. Muller, B.; Guédon, Y.; Passot, S.; Lobet, G.; Nacry, P.; Pagès, L.; Wissuwa, M.; Draye, X. Lateral roots: Random diversity in adversity. *Trends Plant Sci.* **2019**, *24*, 810–825. [[CrossRef](#)]
26. Jia, Z.; von Wirén, N. Signaling pathways underlying nitrogen-dependent changes in root system architecture: From model to crop species. *J. Exp. Bot.* **2020**, *71*, 4393–4404. [[CrossRef](#)]
27. Meier, M.; Liu, Y.; Lay-Pruitt, K.S.; Takahashi, H.; von Wirén, N. Auxin-mediated root branching is determined by the form of available nitrogen. *Nat. Plants* **2020**, *6*, 1136–1145. [[CrossRef](#)]
28. Cai, Q.; Ji, C.; Yan, Z.; Jiang, X.; Fang, J. Anatomical responses of leaf and stem of *Arabidopsis thaliana* to nitrogen and phosphorus addition. *J. Plant Res.* **2017**, *130*, 1035–1045. [[CrossRef](#)]
29. Li, J.; Song, X.; Kong, X.; Wang, J.; Sun, W.; Zuo, K. Natural variation of *Arabidopsis thaliana* root architecture in response to nitrate availability. *J. Plant Nutr.* **2019**, *42*, 723–736. [[CrossRef](#)]
30. Meyer, R.C.; Gryczka, C.; Neitsch, C.; Müller, M.; Bräutigam, A.; Schlereth, A.; Schön, H.; Weigelt-Fischer, K.; Altmann, T. Genetic diversity for nitrogen use efficiency in *Arabidopsis thaliana*. *Planta* **2019**, *250*, 41–57. [[CrossRef](#)]
31. Yan, Z.; Eziz, A.; Tian, D.; Li, X.; Hou, X.; Peng, H.; Han, W.; Guo, Y.; Fang, J. Biomass allocation in response to nitrogen and phosphorus availability: Insight from experimental manipulations of *Arabidopsis thaliana*. *Front. Plant Sci.* **2019**, *10*, 598. [[CrossRef](#)] [[PubMed](#)]
32. Yue, K.; Fornara, D.A.; Li, W.; Ni, X.; Peng, Y.; Liao, S.; Tan, S.; Wang, D.; Wu, F.; Yang, Y. Nitrogen addition affects plant biomass allocation but not allometric relationships among different organs across the globe. *J. Plant Ecol.* **2021**, *14*, 361–371. [[CrossRef](#)]
33. McGrail, R.K.; Van Sanford, D.A.; McNear, D.H., Jr. Trait-based root phenotyping as a necessary tool for crop selection and improvement. *Agronomy* **2020**, *10*, 1328. [[CrossRef](#)]
34. Khan, M.A.E.; Gemenet, D.C.; Villordon, A. Root system architecture and abiotic stress tolerance: Current knowledge in root and tuber crops. *Front. Plant Sci.* **2016**, *7*, 1584. [[CrossRef](#)]
35. Louvieaux, J.; De Gernier, H.; Hermans, C. Exploiting genetic variability of root morphology as a lever to improve nitrogen use efficiency in oilseed rape. In *Engineering Nitrogen Utilization in Crop Plants*; Springer: Berlin/Heidelberg, Germany, 2018; pp. 185–201.
36. Ulas, A.; Erley, G.S.A.; Kamh, M.; Wiesler, F.; Horst, W.J. Root-growth characteristics contributing to genotypic variation in nitrogen efficiency of oilseed rape. *J. Plant Nutr. Soil Sci.* **2012**, *175*, 489–498. [[CrossRef](#)]
37. Guo, X.; Ma, B.; McLaughlin, N.B.; Wu, X.; Chen, B.; Gao, Y. Nitrogen utilisation-efficient oilseed rape (*Brassica napus*) genotypes exhibit stronger growth attributes from flowering stage onwards. *Funct. Plant Biol.* **2021**, *48*, 755–765. [[CrossRef](#)] [[PubMed](#)]
38. Berry, P.M.; Spink, J.; Foulkes, M.J.; White, P.J. The physiological basis of genotypic differences in nitrogen use efficiency in oilseed rape (*Brassica napus* L.). *Field Crops Res.* **2010**, *119*, 365–373. [[CrossRef](#)]
39. Lynch, P.J. Root phenes that reduce the metabolic costs of soil exploration: Opportunities for 21st century agriculture. *Plant Cell Environ.* **2015**, *38*, 1775–1784. [[CrossRef](#)] [[PubMed](#)]
40. Hermans, C.; Porco, S.; Verbruggen, N.; Bush, D. Chitinase-like protein CTL1 plays a role in the root system plasticity in response to multiple environmental signals. *Plant Physiol.* **2010**, *152*, 904–917. [[CrossRef](#)]
41. De Pessemier, J.; Chardon, F.; Juraniec, M.; Delaplace, P.; Hermans, C. Natural variation of the root morphological response to nitrate supply in *Arabidopsis thaliana*. *Mech. Develop.* **2013**, *130*, 45–53. [[CrossRef](#)]
42. Pound, M.P.; French, A.P.; Atkinson, J.A.; Wells, D.M.; Bennett, M.J.; Pridmore, T. RootNav: Navigating images of complex root architectures. *Plant Physiol.* **2013**, *162*, 1802–1814. [[CrossRef](#)] [[PubMed](#)]
43. Hermans, C.; Vuylsteke, M.; Coppens, F.; Craciun, A.; Inzé, D.; Verbruggen, N. The early transcriptomic changes induced by magnesium deficiency in *Arabidopsis thaliana* reveal the alteration of circadian clock genes expression in roots and the triggering of ABA-responsive genes. *New Phytol.* **2010**, *187*, 119–131. [[CrossRef](#)]
44. Hermans, C.; Vuylsteke, M.; Coppens, F.; Cristescu, S.; Harren, F.J.M.; Inzé, D.; Verbruggen, N. System analysis of the responses to long term magnesium deficiency and restoration in *Arabidopsis thaliana*. *New Phytol.* **2010**, *187*, 132–144. [[CrossRef](#)]
45. Malagoli, P.; Laineé, P.; Deunff, E.; Rossato, L.; Ney, B.; Ourry, A. Modeling nitrogen uptake in oilseed rape cv Capitol during a growth cycle using influx kinetics of root nitrate transport systems and field experimental data. *Plant Physiol.* **2004**, *134*, 388–400. [[CrossRef](#)] [[PubMed](#)]
46. Wasson, A.P.; Richards, R.A.; Chatrath, R.; Misra, S.C.; Prasad, S.V.; Rebetzke, G.J.; Kirkegaard, J.A.; Christopher, J.; Watt, M. Traits and selection strategies to improve root systems and water uptake in water-limited wheat crops. *J. Exp. Bot.* **2012**, *63*, 3485–3498. [[CrossRef](#)]
47. Voss-Fels, K.P.; Qian, L.; Parra-Londono, S.; Uptmoor, R.; Frisch, M.; Keeble-Gagnère, G.; Appels, R.; Snowdon, R.J. Linkage drag constrains the roots of modern wheat. *Plant Cell Environ.* **2017**, *40*, 717–725. [[CrossRef](#)]
48. Louvieaux, J.; Spanoghe, M.; Hermans, C. Root morphological traits of seedlings are predictors of seed yield and quality in winter oilseed rape hybrid cultivars. *Front. Plant. Sci.* **2021**, *11*, 568009. [[CrossRef](#)]
49. Hu, Y.; Omary, M.; Hu, Y.; Doron, O.; Hoermayer, L.; Chen, Q.; Megides, O.; Chekli, O.; Ding, Z.; Friml, J.; et al. Cell kinetics of auxin transport and activity in *Arabidopsis* root growth and skewing. *Nat. Commun.* **2021**, *12*, 1657. [[CrossRef](#)]

50. Dupuy, L.X.; Wright, G.; Thompson, J.A.; Taylor, A.; Dekeyser, S.; White, C.P.; Thomas, W.T.B.; Nightingale, M.; Hammond, J.P.; Graham, N.S.; et al. Accelerating root system phenotyping of seedlings through a computer-assisted processing pipeline. *Plant Methods* **2017**, *13*, 57. [[CrossRef](#)] [[PubMed](#)]
51. Xu, Z.; Ma, J.; Lei, P.; Wang, Q.; Feng, X.; Xu, H. Poly- γ -glutamic acid induces system tolerance to drought stress by promoting abscisic acid accumulation in *Brassica napus* L. *Sci. Rep.* **2020**, *14*, 252. [[CrossRef](#)] [[PubMed](#)]
52. Murad, M.A.; Razi, K.; Benjamin, L.K.; Lee, J.H.; Kim, T.H.; Muneer, S. Ethylene regulates sulfur acquisition by regulating the expression of sulfate transporter genes in oilseed rape. *Physiol. Plant.* **2021**, *171*, 533–545. [[CrossRef](#)] [[PubMed](#)]
53. Mairhofer, S.; Pridmore, T.; Johnson, J.; Wells, D.M.; Bennett, M.J.; Mooney, S.J.; Sturrock, C.J. X-ray Computed Tomography of crop plant root systems grown in soil. *Curr. Protoc. Plant Biol.* **2017**, *2*, 270–286. [[CrossRef](#)] [[PubMed](#)]
54. Pfeifer, J.; Kirchgessner, N.; Colombi, T.; Walter, A. Rapid phenotyping of crop root systems in undisturbed field soils using X-ray computed tomography. *Plant Methods* **2015**, *11*, 41. [[CrossRef](#)] [[PubMed](#)]
55. Watt, M.; Moosavi, S.; Cunningham, S.C.; Kirkegaard, J.A.; Rebetzke, G.J.; Richards, R.A. A rapid, controlled-environment seedling root screen for wheat correlates well with rooting depths at vegetative, but not reproductive, stages at two field sites. *Ann. Bot.* **2013**, *112*, 447–455. [[CrossRef](#)] [[PubMed](#)]
56. Leijten, W.; Koes, R.; Roobeek, I.; Frugis, G. Translating flowering time from *Arabidopsis thaliana* to Brassicaceae and Asteraceae crop species. *Plants* **2018**, *7*, 111. [[CrossRef](#)]
57. Stephenson, P.; Stacey, N.; Brüser, M.; Pullen, N.; Ilyas, M.; O'Neill, C.; Wells, R.; Østergaard, L. The power of model-to-crop translation illustrated by reducing seed loss from pod shatter in oilseed rape. *Plant Reprod.* **2019**, *32*, 331–340. [[CrossRef](#)]
58. Li, X.; Zeng, R.; Liao, H. Improving crop nutrient efficiency through root architecture modifications. *J. Integr. Plant Biol.* **2016**, *58*, 193–202. [[CrossRef](#)] [[PubMed](#)]
59. Thorup-Kristensen, K.; Kirkegaard, J. Root system-based limits to agricultural productivity and efficiency: The farming systems context. *Ann. Bot.* **2016**, *118*, 573–592. [[CrossRef](#)]
60. Pierret, A.; Maeght, J.; Clément, C.; Montoroi, J.; Hartmann, C.; Gonkhamdee, S. Understanding deep roots and their functions in ecosystems: An advocacy for more unconventional research. *Ann. Bot.* **2016**, *118*, 621–635. [[CrossRef](#)]
61. Van der Bom, F.J.T.; Williams, A.; Bell, M.J. Root architecture for improved resource capture: Trade-offs in complex environments. *J. Exp. Bot.* **2020**, *71*, 5752–5763. [[CrossRef](#)]
62. Gu, M.G.; Hu, X.; Wang, T.; Xu, G. Modulation of plant root traits by nitrogen and phosphate: Transporters, long-distance signaling proteins and peptides, and potential artificial traps. *Breed Sci.* **2021**, *71*, 62–75. [[CrossRef](#)] [[PubMed](#)]
63. Ohkubo, Y.H.; Tanaka, M.; Tabata, R.; Ogawa-Ohnishi, M.; Matsubayashi, Y. Shoot-to-root mobile polypeptides involved in systemic regulation of nitrogen acquisition. *Nat. Plants* **2017**, *3*, 17029. [[CrossRef](#)] [[PubMed](#)]